NASA

Technical Memorandum **79684**

Nonlinear Stability of Solar Type III Radio Bursts: II. Application to Observations Near 1 A. U.

Melvyn L. Goldstein,
Robert A. Smith
Konstantinos Papadopoulos,

December 1978

National Aeronautics and
Space Administration

Goddard Space Flight Center
Greenbelt, Maryland 20771

ABSTRACT

A set of rate equations including strong turbulence effects and anomalous resistivity are solved using parameters which model several solar type III bursts. The electron exciters of these bursts have been detected at earth orbit. The analysis has enabled us to provide quantitative comparisons between several of the observed phenomena and the theory. Using an analytic model for the time evolution of the energetic electron exciter, we find that the exciter distributions observed at 1 AU are unstable to the excitation of the linear bump-in-tail instability, amplifying Langmuir waves above the threshold for the oscillating two stream instability (OTSI). The OTSI, and the attendant anomalous resistivity produce a rapid spectral transfer of Langmuir waves to short wavelengths, out of resonance with the electron exciter. Further energy loss of the beam is thus precluded. The various parameters needed to model the bursts are extrapolated inside 1 AU with similar results. Again, the OTSI is excited and decouples the electron beam from the Langmuir radiation. Reabsorption of the Langmuir waves by the beam is shown to be unimportant in all cases, even at 0.1 AU.

The theory provides a natural explanation for the observed relationship between radio flux, I, and the electron flux, J_E. When the OTSI is weakly excited the theory predicts that $I \propto J_E$, as observed; while for stronger bursts, the theoretical result is $I \propto J_E^{\alpha}$, with $\alpha \approx 2.4$. We find that the value of α is only weakly dependent on variations in beam density and the spectral index of the exciter distribution function. In all cases the theoretical results agree closely with the observed values.

I. INTRODUCTION

Observations of solar type III bursts have reached a level of sophistication which permits both qualitative and quantitative comparison between theory and experiment. In the accompanying paper (Smith, Goldstein and Papadopoulos 1979, henceforth referred to as Paper III--Papers I and II being, respectively, Papadopoulos, Goldstein and Smith 1974 and Smith, Goldstein and Papadopoulos 1976), we presented a theory of strong plasma turbulence as it applies to type III burst phenomena. In the present paper we extend the analysis of Paper III in an effort to provide quantitative comparisons between the strong turbulence theory and many aspects of type III phenomenology.

In §II, the basic equations of the theory are solved numerically for parameters appropriate to several specific bursts. The solutions demonstrate the importance of the role played by the oscillating two stream instability (OTSI) and anomalous resistivity in decoupling the electron exciter from the plasma turbulence. Reabsorption, included in the analysis, is shown to be unimportant in all calculations at all heliocentric distances.

The computed levels of Langmuir turbulence agree well with the recent reports by Gurnett and Anderson (1976 and 1977) of intense sporadic bursts of electrostatic noise observed in association with type III bursts. The predicted intensity of electromagnetic noise resulting from the Langmuir turbulence is found to be comparable to the observed levels. In addition, we show that the puzzling correlation between electron flux and radio intensity (Fitzenreiter, Evans and Lin 1976) has a natural explanation in the functional dependence of the OTSI growth rate on levels of Langmuir energy density.

II. NUMERICAL CALCULATIONS

The model rate equations describing the spectral evolution of electron plasma oscillations, including the effects of the linear beam-plasma instability, the oscillating two stream parametric instability and anomalous resistivity were first derived in Paper II and were more fully described in Paper III. The integration of the system of equations (III-3.44)-(III-3.47) is the subject of this section. [Roman numerals refer to the paper in which the equations are found.] Definitions of the various growth and damping rates (γ_L, γ_{OTS}, γ_{NL} and γ_L) can also be found in Paper III. The integration required discretizing wavenumber space, or equivalently - phase velocity. Thus, there were of the order of 200 coupled non-linear differential equations integrated in time over the interval $-0.7 \lesssim \omega/kc \lesssim 0.7$.

The starting condition (t=0) was the arrival at the location of interest (a point between 0.1 and 1 AU) of energetic electrons with streaming velocities centered near 0.7c. The exact velocity distribution of the electron beam at that location was given by the beam evolution model described in §IV of Paper III. That beam evolution model was first constructed for a single event; it has but one free parameter, L--the path length traveled by the exciter. By varying L, the time behavior of the model at 1 AU could be adjusted to fit observations by Lin and coworkers of several different bursts (Lin 1974, and Fitzenreiter, Evans and Lin 1976). In all cases, the observers found that at first only the fastest particles were detected (with energies $\sim$100 keV). This was followed over an extended period of time ($\sim$20-30 minutes) by the arrival of an increasing flux of slower particles (cf. Figure 1). The long time over which the electron flux was observed to increase indicates that the particles experienced significant amounts of pitch-angle scattering; more

than can be accounted for by interactions with Langmuir turbulence excited by the bump-in-tail instability. In constructing our model of the beam evolution (cf. Paper III), we took this into account by requiring that our phenomenological model reproduce the time behavior of the electron flux that Lin and coworkers observed. The physical origin of this enhanced pitch-angle scattering is probably due to the interaction of the electrons with the magnetic fluctuations known to permeate the interplanetary medium. In this context, it is well to point out that calculations involving solutions to the time dependent quasilinear (i.e., weak turbulence) equations have been published by Takakura and Shibahashi (1976), Takakura (1977), and Magelssen and Smith (1977) in which the effects of magnetic pitch-angle scattering were ignored.

In Magelssen and Smith's calculation, which attempted to model the type III burst of 16 May 1971, the calculated electron distribution evolved from 100 keV to below 20 keV in less than 5 minutes (v. Figure 13 of their paper). As a consequence of this rapid evolution of the exciter distribution, reabsorption of the linerly excited Langmuir waves was found to be very important. In a situation in which the flux of low energy electrons is rapidly increasing with time, reabsorption occurs as the peak of the electron distribution function, initially located at rather large velocities, shifts to lower velocities. Langmuir waves that had been initially excited when the slope of the electron distribution function was positive soon find themselves interacting with the portion of the distribution with negative slope. The waves are then quickly damped or reabsorbed.

In our analysis reabsorption will be unimportant as long as the beam evolves slowly compared to the time necessary for the OTSI to effect a spectral transfer of the Langmuir radiation to large wavenumbers, out of resonance with the exciter distribution. In situations where the beam

evolution is as rapid as that considered by Magelssen and Smith (1977), reabsorption can be an important effect, however, as shown in Figure 1, Lin's observations indicate that more than 30 minutes actually elapsed before the peak of the distribution evolved to 30 keV. Consequently, Magelssen and Smith's calculation greatly overemphasizes the effects of reabsorption. As we show below, the OTSI produces a spectral transfer of the Langmuir radiation on time scales of less than a second, and thus reabsorption is unimportant in our analysis.

As an initial condition in our calculations, the Langmuir and ion waves are taken to be in thermal equilibrium with the solar wind plasma, the equilibrium energy density of Langmuir waves being the enhanced noise levels produced by the suprathermal tails of the electron distribution function (v. eq. III-3.41).

The rate equations were integrated using a predictor-corrector algorithm with variable step-size (Eiserike and Silver 1971). For each of several bursts the code was run at heliocentric distances ranging from 0.1 to 1.0 AU. In the following discussion, the results of the calculations are described for each burst in turn; first for parameters which model observations at 1 AU and then for parameters which model observations between 0.1 and 1 AU.

(a) <u>The burst of 16 May 1971 at 1 AU.</u>

This was an isolated and fairly intense burst (reaching nearly 10^{-17} W m^{-2} Hz^{-1}--Fitzenreiter, Evans and Lin 1976) observed by instruments on both the IMP-6 spacecraft and the Apollo 16 subsatellite. These two spacecraft were able to simultaneously measure both the radio and particle fluxes. [Electron spectra, estimates of the beam densities, and estimates of the path lengths

traversed by the beam before reaching 1 AU for this and the other bursts were kindly provided to us by R. P. Lin and R. J. Fitzenreiter (also see Lin 1974).]

The local plasma frequency, f_{pe}, at 1 AU on May 16, 1971 was about 30 kHz. Electrons with energies in excess of 100 keV and radio noise at 55 kHz ($\approx 2f_{pe}$) were first detected by instruments on IMP-6 at 1305 UT (see Figure 1, which is taken from Lin et al. 1973). By 1335 UT the radio noise had reached its maximum and little further evolution of the electron spectrum was observed. Between 1305 and 1312 UT the peak of the electron spectrum had shifted from several hundred keV to about 80 keV. Subsequent evolution was slow, and it was not until 1324 UT that the peak had moved to about 50 keV. By 1332 UT the peak was at 40 keV, and had evolved to 30 keV by 1335 UT. At later times no clearly defined peak was present. Thus, thirty minutes elapsed between the time that 100 keV electrons were first observed and the time that the peak of the spectrum had moved down to 30 keV. As discussed above, our model of the beam is constructed to have this slow evolution.

For the burst on 16 May 1971 (at 1 AU), the path length L was estimated to be 1.5 AU. The ratio of the density of the beam to that of the solar wind was $\eta \approx 5\times10^{-6}$, and the spectral index of the electron distribution was $\zeta \approx 4.6$. These parameters are summarized in Table 1 for this and all other calculations. Below the peak velocity, $\beta_p(t)$, the distribution function, $f(\beta)$ had a positive slope throughout the 30 minutes between 1305-1335 UT. With these parameters, the rate equations were integrated and the evolution of the plasma instabilities followed in some detail.

The solution is presented graphically in Figure 2, where $f_T(\beta)$, $W(+k)$, $W(-k)$, and $(\delta n/n)^2 = S(k)(k\lambda_e)^2$ are plotted on a logarithmic scale against $v_{ph} = \omega_k/kc$ at various times (Fig. 2a-2f).

Initially the linearly unstable beam produces resonant plasma waves (indicated by cross hatching in Fig. 2a) that grow until the turbulence level exceeds the threshold of the OTSI (eq. III-3.29) At this time $W \approx 1 \times 10^{-5}$ (corresponding to an electric field of 2 mV/m). With the onset of the OTSI, aperiodic ion waves are excited (the gray shading in Fig. 2c-2f) at the growth rate given by equation (III-3.28) This is also the rate at which the "pump" waves earlier excited by the linear instability are scattered to shorter wavelength "daughter" waves propagating parallel and antiparallel to the beam (Fig. 2b-2d). If there were no other physical processes operating, the pump waves would saturate near the threshold value of $W \approx 10^{-5}$. Although this saturation level is well below that expected on the basis of weak turbulence theory ($W \sim 1$), resonant energy exchange between the beam and the pump waves would continue, eventually leading to substantial deceleration of the beam.

However, the OTSI does not stabilize at this enhanced level; for as the ion turbulence grows, the ion density fluctuations modify the Bohm-Gross dispersion relation so that the threshold of the OTSI is lowered (cf. eq. III-3.34). This further reduces the energy in pump waves (Fig. 2e). Finally, the a-c anomalous resistivity associated with the correlated ion fluctuations scatters all long wavelength Langmuir waves to short wavelengths (Fig. 2f). In our calculations the collapse to short wavelengths ceases when Landau damping by the thermal electrons balances the scattering. At this point the process has stabilized. The electron beam is now completely decoupled from the plasma waves, and no further energy exchange will take place between the beam and the radiation field. If we were to continue the calculation, which we have not done for reasons of economy, we would expect that gradually the ion fluctuations and Langmuir waves would simultaneously decay. This is a process that has not been fully investigated theoretically, but should take

place on the time scale of ion Landau damping (eq. III-3.39). Eventually, following the decay of the ion fluctuations, the linear instability could begin again. Such a cyclic process, similar to relaxation oscillations, would continue until the electron beam merges with the ambient solar wind electron distribution, at which time the total distribution function $f_T(\beta)$ would not have a positive slope. [We reported similar behavior in an earlier version of these calculations (Paper II). Recently, H. Rowland has observed the same cyclic phenomenon using Vlasov type simulations for both electrons and ions (Rowland, private communication).] Merging of the exciter distribution function with the solar wind was observed by Gurnett and Frank (1975) during the type III burst on 5 November 1974. Another mechanism for ending the instability would be the disappearance of the velocity space anisotropy. In fact, this latter possibility seems more consistent with observations of the anisotropy made by Lin during the 16 May event (Lin, private communication).

Little more than 0.1s elapsed between the time of OTSI threshold was reached and the final stabilization of the various instabilities. In 0.1s the electron distribution is essentially constant, vindicating our claim that neither reabsorption nor quasilinear relaxation is important. Even the 2.8 minutes during which the linear instability operates at 1 AU is insufficient time for the beam to reabsorb an appreciable amount of wave energy. We reiterate that our calculation <u>includes</u> the damping of the waves (or reabsorption) at all phase velocities for which $\partial f/\partial\beta<0$ (cf. eq. III-3.43).

(b) <u>The burst of 28 February 1972 at 1 AU.</u>

This burst was less intense than the one on 16 May 1971, the electron flux was lower, the distribution function had a softer spectum (ζ=10.4), but,

nonetheless, the beam was relatively dense ($\eta \approx 1.4 \times 10^{-4}$). The plasma frequency at 1 AU was $\sim$30 KHz, and the ambient electron temperature was $\approx 1.2 \times 10^{5}$°K. The beam is estimated to have traversed a path length L=1.9 AU. At 1 AU stabilization proceeds in much the same way it did for the 16 May 1971 event (Fig. 3a-3c). However, because ζ is larger, threshold for the OTSI occurs at smaller $\beta_p \approx 0.31$ with $W \approx 5 \times 10^{-5}$.

As before, stabilization proceeds rapidly once OTSI threshold is attained, and neither reabsorption nor quasilinear relaxation are important. Figure 3a shows the pump waves near threshold; in Figure 3b the OTSI has scattered most of those waves to lower phase velocities (both parallel and anti-parallel to the electron beam); and in Figure 3c stabilization is complete. Note that the electron flux at stabilization is significantly smaller for this and the 25 May 1972 burst, discussed below, than it was for the burst on 16 May 1971 (Fig. 2).

(c) The burst of 25 May 1972.

This was similar in some respects to the one on 28 February 1972 just discussed. The spectrum was again soft (ζ=6.4), the electron and radio fluxes were rather modest compared to the 16 May 1971 event, and the electron beam was even less dense ($\eta \approx 5.6 \times 10^{-5}$) than on 28 February 1972. The ambient electron temperature was 1.2×10^{5}°K, L=1.5 AU, and f_{pe}=22 KHz. At 1 AU the OTSI threshold was reached at $\beta_p \approx 0.33$ and $W \approx 4 \times 10^{-5}$. Stabilization again proceeded quickly (Fig. 3d-3f).

(d) Variation with heliocentric distance.

Our discussion has thus far been confined to calculations using parameters

characteristic of conditions at 1 AU, because it is only at 1 AU that simultaneous radio and particle data have thus far been available. Observations of plasma and radio waves, but not simultaneous electron measurements, have been published following the HELIOS 1 and 2 missions to 0.45 AU. This has prompted us to investigate solutions to the rate equations at various heliocentric distances between 0.1 and 1 AU.

At 0.5 AU, for the 16 May 1971 event, we took the plasma frequency to be 60 KHz, L=0.7 AU, and assumed that η and ζ were constant with heliocentric distance--(Table 1). The results are qualitatively similar to those obtained at 1 AU, although the threshold energy density is now $W=3\times10^{-5}$ (corresponding to an electric field of $\sim$4 mV/m). Because one is closer to the corona, the electron distribution evolves more rapidly so that the peak of the spectrum is near 0.45c when the OTSI threshold is reached. The more rapid beam evolution at smaller heliocentric distances implies that reabsorption of the electron oscillations by the beam probably plays a somewhat more important role in the inner solar system than at 1 AU. Nonethless, as shown in Figure 4a-4c, stabilization proceeds via the OTSI and anomalous resistivity, and not by reabsorption. [Note that in Figures 4 and 5, for reason of economy, the calculation have not been carried through to the point where the OTSI is completely stabilizaed by anomalous resistivity (cf. Figs. 2f, 3c and 3f).]

Figures 4d-4e show the results of integrating the rate equations for the 16 May 1971 burst at 0.1 AU. For this calculation f_{pe}=300 KHz and L=0.1 AU. Stabilization proceeds as before via the OTSI, and again reabsorption is unimportant. At threshold, $W=1\times10^{-4}$ and β_p=0.3c.

Similar calculations were performed for the 25 May 1972 and 28 February 1972 events at both 0.5 and 0.1 AU. These results are shown in Figure 5 (0.5 AU) and Figure 6 (0.1 AU). Again, these bursts reached the OTSI threshold at

somewhat lower electron velocities than was the case with the more intense burst of 16 May 1971 (cf. Fig. 4). Nonetheless, even at 0.1 AU reabsorption is not significant, and the beam becomes decoupled from the Langmuir turbulence after anomalous resistivity stabilizes the OTSI.

These three bursts (16 May 1971, 25 May 1972 and 28 February 1972) are the only ones for which we had electron data sufficiently complete to provide the parameters needed in the beam evolution model, viz. L, η, and ζ. They are included in the events analyzed by Fitzenreiter, Evans and Lin (1976). In that analysis, Fitzenreiter, et al. discovered a relationship between the radio flux, I, and electron flux, J_E. When J_E was less than 100 $(cm^2 \cdot s \cdot ster)^{-1}$, I and J_E were related by $I(2\omega_e) \propto J_E^{\alpha}$ with $\alpha=1$. For $J_E>100$ $(cm^2 \cdot s \cdot ster)^{-1}$, $I(2\omega_e) \propto J_E^{\alpha}$ with $\alpha=2.4$.

The three bursts we were able to model represent examples in which was either of order 2.4 or changed from 1 to 2.4 during the event. The 16 May 1971 burst was an example for which $\alpha=2.6$ from the onset of the burst at 1 AU (1305 UT). For both the 28 February and 24 May 1972 events, J_E was less than 100 $(cm^2 \cdot s \cdot ster)^{-1}$ for some ten minutes after onset, and $\alpha=1$. Subsequently, J_E exceeded 100 $(cm^2 \cdot s \cdot ster)^{-1}$ and α increased to about 2.4. We will return to discuss these two classes of events in more detail following the discussion of solitons, which follows.

III. SOLITONS

In order to give a theoretical description of the electromagnetic radiation properties of these bursts and the correlation between J_E and I, we must consider the spatial structure of the collapsed short wavelength plasma oscillations represented in Figure 2f.

A comparison of Figures 2a and 2f illustrates the collapse of the long wavelength pump wave into short wavelength daughter waves. As pointed out by Manheimer and Papadopoulos (1975), the equations that describe the OTSI are the Fourier representations of those that describe soliton formation. In configuration space the pump waves comprise a wavepacket with dimensions $\Delta z = 1/\Delta k_o = 1200\lambda_e = 8$ km with $\lambda_e = 700$ cm at 1 AU. Following collapse, the scale length of the solitons, Δx_s, is $\Delta x_s = 50\lambda_e = [illegible]$ km and W has reached nearly 10^{-2}. This is something of an overestimate because our numerical calculation does not take into account the effect of the magnetic field in inhibiting collapse in the transverse directions. When $W \ll 1$ each wavepacket collapses into one soliton, so the spacing between solitons is approximately Δz.

Soliton formation can be investigated directly from equations (III-3.11)-(III-3.12) (Zakharov 1972, Rudakov 1973). Papadopoulos and Freund (1978) have argued that the solitons collapse only in the direction parallel to $\underline{B}$, in which case the energy density in the soliton can be estimated to be (Kingsep, Rudakov, and Sudan 1973, Degtyarov, Zakharov, and Rudakov 1976).

$$W = 12(k\lambda_e)^2 (1 + T_e/T_i) = 24(k\lambda_e)^2$$

With $k\lambda_e = 5 \times 10^{-2}$ (cf. Fig. 2f), one finds $W \gtrsim 10^{-2}$, which corresponds to an electric field on 60 mV/m.

Until recently, there has been little experimental evidence that such collapsed, intense electric fields accompany type III bursts. The reason is clear. In a 400 km/s solar wind, a 350m soliton is convected past a 30m dipole antenna in little more than a millisecond. Plasma wave experiments on spacecraft have been designed with electronic response times no faster than 20ms (D. A. Gurnett, private communication) so that the likelihood of detecting a fully collapsed soliton along its parallel dimension is small.

Papadopoulos and Freund (1978) noted that because there is little or no collapse along the transverse direction, solitons might be detected as the transverse dimension, $L_\perp$, is swept past an antenna. Depending on the ratio ω_e/Ω_e, this size might be connected with either the beam electron Larmor radius, or the transverse correlation length of the instability, $(v_g/\gamma)_\perp = v_g/\gamma_L$. For example, at 0.45 AU, $L_\perp \simeq 3(V_e/V_b)\cdot(V_e/\gamma_L) \simeq 20\text{-}100$ km, so that the transverse size of a soliton might take longer than 60ms to convect past a spacecraft, and would then be detectable. While the two HELIOS spacecraft were near 0.45 AU, Gurnett and Anderson (1976, 1977) did report observations of intense, sporadic bursts of plasma oscillations in association with four type III bursts. The intense plasma oscillations at ω_e ($E \sim 15$ mV/m) were observed only after the electromagnetic radiation at $2\omega_e$ had reached its maximum and started to decay.

Because the strong bursts of plasma oscillations often lasted for 1/3s of longer, Gurnett and Anderson could not have observed a fully collapsed soliton convecting past the spacecraft as long as the magnetic field was approximately parallel to the flow direction of the solar wind. However, this observation is consistent with the transverse dimension, X, of a soliton being convected past the spacecraft if 25 km $\lesssim$ X $\lesssim$ 90 km, which satisfies the requirement that X be greater than R_b (Papadopoulos and Freund 1978). When detailed magnetic field data from the HELIOS magnetometer experiments becomes available it

should be possible to determine the orientation of solitons when the spiky turbulence was observed.

An alternative interpretation is possible, though without additional analysis it is at present only a suggestion, viz., that after the pump wave has been depleted, the collapse wave packet begins to spread diffusively at its group velocity. At 0.45 AU, $\lambda_e \simeq 400$ cm and $v_g \simeq 10^7$ cm/s. In 1s the packet would diffuse to a size of 7×10^7 cm, which would take $\sim$1/4s to convect past the antenna system. However, at these dimensions, expanding solitons would start interacting with each other. This situation has not been investigated and is beyond the scope of the present paper.

(a) Radiation from Solitons

A soliton is a spatially confined structure in which intense electrostatic fields oscillate at frequencies very close to ω_e. As pointed out by Papadopoulos and Freund (1978), such fields will produce a second order current $\underline{j}_2 = en_1\underline{v}_1$, where n_1 is the density perturbation consistent with Poisson's equation, and $\underline{v}_1$ is the velocity perturbation produced by the soliton electric field. If that field has the form (in cylindrical coordinates)

$$\underline{E}(\underline{r},t) \simeq \hat{e}_z\, E(r,z)\, \sin(\omega_e t)$$

then (Papadopoulos and Freund 1978)

$$\underline{j}_2 = \frac{-\hat{e}_z e}{8\pi m\omega_e}\left(E\,\frac{\partial E}{\partial z}\right)\sin(2\omega_e t)$$

Note that radiation will be produced directly at $2\omega_e$. For the spatial structure of a soliton one can take (Degtyarov el al. 1976, Papadopoulos and Freund 1978)

$$E(r,z) = E_o e^{-r/L} \operatorname{sech}(k_o z)$$

Papadopoulos and Freund (1978) then find that the total volume emissivity, $J(2\omega_e)$ is

$$J(2\omega_e) = \left(\frac{3\sqrt{3}}{8}\right)\left(\frac{v_e}{c}\right)^3\left(\frac{cE_o^2}{8\pi\Delta z}\right)\left(\frac{1}{k_o L}\right)^2 \tag{3.1}$$

where, again, Δz is the parallel dimension of the linearly unstable wave packet and $k_o = \sqrt{3}\omega_e/c$ is the wavelength of the electromagnetic wave at $2\omega_e$. In writing equation (3.1) we have assumed that $k_o^2 L^2 >> 4$, as it is throughout the interplanetary medium. The intensity of emission just outside a spherical shell of radius R and thickness ΔR centered on the sun is (Gurnett and Frank 1975)

$$I \propto \frac{JR}{(2\omega_e/2\pi)} \tag{3.2}$$

Equations (3.1) and (3.2) can be evaluated as the rate equations are integrated. For the 16 May 1971 burst, at the time of soliton formation at 1 AU (Fig. 2f), we find that $I \sim 1\times10^{-17}$ W m^{-2} s^{-1} with $\Delta z \approx 3(v_b/v_e)\lambda_e \approx 2$ km and $L \approx 24$ km. This is close to the peak intensity that was observed during that event at 55 KHz. As stated above, our calculation probably over estimates $E_o^2/8\pi$ in the soliton, and so, coupled with the uncertainties in determining the other parameters of the model, this seems to be quite satisfactory agreement.

(b) Radio and Electron Flux Relationship.

As we mentioned, Fitzenreiter, Evans and Lin (1976) discovered a strong correlation between simultaneously observed radio and electron fluxes.

Papadopoulos and Freund (1978) pointed out that this correlation results from the scaling of $W(k_o)$ with γ_{OTS}. For the parameter range of interest in the solar wind, this scaling law is (Papadopoulos 1975, Rowland 1977)

$$W(k_o) \propto \gamma_{OTS} \qquad m/M > W(k_o) > W_T$$

$$W(k_o) \propto \gamma_{OTS}^2 \qquad W(k_o) > m/M \tag{3.3}$$

The growth rate used in our computations (eq. III-3.28) follows this scaling law very closely (Fig. 7). In fact, the asymptotic regime $W(k_o) \propto \gamma_{OTS}^2$ is reached for values of $W(k_o)$ somewhat less than m/M.

When the OTSI stabilizes the beam plasma instability, $\gamma_{OTS} \propto \gamma_L$, and $\gamma_L \propto n_b$. With $I(2\omega_e) \propto W(k_o)$ (eq. 3.1 and 3.2), one has $I(2\omega_e) \propto n_b$ or n_b^2. The electron flux, J_E, is in turn proportional to $n_b \langle v \rangle$, where $\langle v \rangle$ is the velocity of the peak of the exciter distribution--it is that part of the electron beam that drives the linear instability. Thus, with $f \propto v^{-\zeta}$, one has $n_b \propto J_E^{[(1-\zeta)/(2-\zeta)]}$ so that

$$I(2\omega_e) \propto J_E^{(1-\zeta)/(2-\zeta)} \qquad m/M > W(k_o) > W_T$$

or

$$I(2\omega_e) \propto J_E^{2(1-\zeta)/(2-\zeta)} \qquad W(k_o) > m/M \tag{3.4}$$

The 16 May 1971 event exhibited no transition and α was 2.63 during the entire event. We noted earlier that for this event $\zeta \simeq 4.6$, so that, from equation (3.4) we calculate $\alpha = 2.77$.

On 28 February 1972 the electron spectrum had a slope of $\zeta=10.4$, which yields $\alpha=2.24$ late in the event. Fitzenreiter et al., observed $\alpha=0.84$ at $J_E<100$ $(cm^2 \cdot s \cdot ster)^{-1}$ and $\alpha=2.38$ at larger J_E.

Similarly, the 25 May 1972 burst had $\zeta=6.4$, implying theoretical values of $\alpha=1.23$ and 2.46, while $\alpha=0.92$ and 2.54 were observed. Not only are computed values of α remarkably close to those observed but we also find that the relative order is accounted for, i.e., α is largest on 16 May 1971 and smallest on 28 February 1972. These results are summarized in Figure 8.

The scaling $W(k_o) \sim \gamma_{OTS}$ implies that α should not be less than one. From Figure 7, however, it is clear that very close to threshold, $W(k_o) \sim \gamma_{OTS}^{\nu}$ with $\nu<1$. Thus, for bursts which initially only weakly excite the OTSI, one does expect values of $\alpha<1$. In fact our numerical calculations confirm that for both of the 1972 bursts (28 February and 25 May), $W(k_o)$ does not exceed W_T by nearly as much as it did during the 16 May 1971 burst.

IV. CONCLUSIONS

In this series of papers we have sought to demonstrate that the physics of solar type III radio bursts is a manifestation of strong plasma turbulence processes. The oscillating two stream instability together with anomalous resistivity provide the means by which electrons with energies from tens of keV up to the order of 100 keV are able to traverse distances greater that 10^{13}cm with only modest energy losses. In modeling the nonlinear processes by means of the rate equations derived in Paper II we have been able to study type III bursts using parameters typical of those observed in the solar wind. This is often difficult to do in numerical simulations of parametric instabilities, primarily because of the very low beam densities found in the interplanetary medium ($n \approx 10^{-4}$-10^{-6}). We have found that for the parameter range we were able to model, electron beams will produce levels of Langmuir turbulence which exceed the threshold for excitation of the OTSI. Furthermore, these levels are reached on time scales that are rapid compared to the time scale over which the peak of the electron distribution function of the stream evolves to lower velocities. Consequently, the spectral transfer of Langmuir radiation to large wavenumbers (small wavelengths), occurs rapidly. The phase velocity of the radiation then lies in a region of phase space in which there are few if any exciter electrons--the electron beam then propagates without further energy loses. Because of the relatively slow time evolution of the electron exciter, reabsorption of the Langmuir radiation was of minor importance.

As pointed out by Papadopoulos and Freund (1978), theories based on weak turbulence predict far higher intensities of radio noise (by up to three orders of magnitude) than is observed. In contrast, because electromagnetic radiation from solitons is proportional to $E^2/8\pi$ (rather than $E^4/(8\pi)^2$), the radiation levels computed are close to those observed. Furthermore, the

should be possible to determine the orientation of solitons when the spiky turbulence was observed.

An alternative interpretation is possible, though without additional analysis it is at present only a suggestion, viz., that after the pump wave has been depleted, the collapse wave packet begins to spread diffusively at its group velocity. At 0.45 AU, $\lambda_e \approx 400$ cm and $v_g \approx 10^7$ cm/s. In 1s the packet would diffuse to a size of 7×10^7 cm, which would take $\sim$1/4s to convect past the antenna system. However, at these dimensions, expanding solitons would start interacting with each other. This situation has not been investigated and is beyond the scope of the present paper.

(a) Radiation from Solitons

A soliton is a spatially confined structure in which intense electrostatic fields oscillate at frequencies very close to ω_e. As pointed out by Papadopoulos and Freund (1978), such fields will produce a second order current $\underline{j}_2 = en_1\underline{v}_1$, where n_1 is the density perturbation consistent with Poisson's equation, and $\underline{v}_1$ is the velocity perturbation produced by the soliton electric field. If that field has the form (in cylindrical coordinates)

$$\underline{E}(\underline{r},t) = \hat{e}_z\, E(r,z)\, \sin(\omega_e t)$$

then (Papadopoulos and Freund 1978)

$$\underline{j}_2 = \frac{-\hat{e}_z e}{8\pi m\omega_e}\left(E\,\frac{\partial E}{\partial z}\right)\sin(2\omega_e t)$$

Note that radiation will be produced directly at $2\omega_e$. For the spatial structure of a soliton one can take (Degtyarov el al. 1976, Papadopoulos and Freund 1978)

theory naturally accounts for the observed predominance of second harmonic radiation.

Perhaps the most convincing evidence of the importance of strong turbulence effects, and in particular, of the OTSI, is the ability of the theory to account for the observed correlation between the radio and electron fluxes--$I(2\omega_e) \propto J_E^{\alpha}$, with $\alpha \simeq 1$ for weak bursts, and $\simeq 2.4$ for stronger ones. Within the context of the theory, bursts which strongly excite the OTSI will amplify Langmuir waves well above threshold, into the scaling region where $W \sim \gamma_{OTS}^2$ and $\alpha \simeq 2.4$; while for weaker bursts $W \sim \gamma_{OTS}$ and $\alpha \simeq 1$.

There remains one outstanding problem in the theory of type III bursts which we have not addressed; namely, the decay phase. The problem is twofold. In the first place, the decay of the electromagnetic radiation is observed to be exponential to a high degree and for a long time. The second feature is that the product of the decay time and the observed frequency is nearly constant over four decades in frequency. Previous attempts to provide an explanation for the decay have invoked either collisional damping of the plasma waves (Jaeger and Westfold 1949, and Malville 1962), or Landau damping (Zaitsev, Mityakov and Rappoport 1972, and Harvey and Aubier 1973). However, at decametric and hectometric frequencies collisional damping is slower (by nearly an order of magnitude at 100 KHz) than the observed decay rate; and were Landau damping the dominant mechanism, radio bursts should cease abruptly after the intensity has decayed by only a few e-foldings (Harvey and Aubier 1973, and Aubier 1974). To develop a complete theory of the decay phase would require an understanding of how solitons decay in time, which is an unsolved problem in strong plasma turbulence theory, and is beyond the scope of the present analysis.

The authors wish to acknowledge R. P. Lin and R. J. Fitzenreiter for providing the detailed particle and radio flux data which were invaluable in constructing the beam evolution model described above. We thank R. G. Stone, J. Fainberg, W. Weber, D. A. Gurnett, P. J. Kellogg, H. Freund, H. Rowland, G. de Genouillac, D. Nicholson, and M. Goldman for stimulating discussions. E. Sullivan provided invaluable assistance with numerical computations. The work of K. Papadopoulos was supported by the Office of Naval Research.

FIGURE CAPTIONS

Figure 1. After Lin et al. (1973). Electron spectra are shown at various times during the type III burst of 16 May 1971.

Figure 2. Results of a numerical solution of the rate equations that describe the OTSI. Parameters were chosen to model the 16 May 1971 event at 1 AU. For this calculation, L=1.5 AU, $\eta=5\times10^{-6}$, $\zeta=4.6$ and $f_{pe}=30$ KHz. Panel (a) shows, f_T, the distribution function of the solar wind and the linearly unstable exciter beam, as well as the Langmuir wave energy density, W(+k)--the diagonally striped histogram. W(k) has nearly reached W_T, the OTSI threshold. Panels (b-f) illustrate subsequent stages of excitation and stabilization of the OTSI. Ion oscillations are depicted by the gray shading. Times are computed from the start of the numerical calculations. Calculated values of the electron flux are given in panels a, d, and f.

Figure 3. Similar to Figure 2. Panels (a-c) show results using parameters for the 28 February 1972 burst at 1 AU. In this calculation $\zeta=10.4$, L=1.9 AU, $\eta=1.4\times10^{-4}$ and $f_{pe}=30$ KHz. In panels (d-f) a similar calculation is shown for the 25 May 1972 burst, for which $\zeta=6.4$, L=1.5 AU, $\eta=5.6\times10^{-5}$ and $f_{pe}=22$ KHz.

Figure 4. Panels (a-c) show results using parameters for the 16 May 1971 burst at 0.5 AU. In this calculation L=0.7 AU and $f_{pe}=60$ KHz, while η and ζ were unchanged from the 1 AU calculation. Panels (d-f) model the burst at 0.1 AU for which L=0.1 AU and $f_{pe}=300$ KHz. Note that stabilization proceeds as before via the OTSI, and reabsorption is unimportant.

Figure 5. Results at 0.5 AU for two bursts. In panels (a-c) the 25 May 1972 burst is modeled using L=0.7 AU and f_{pe}=44 KHz. Panels (d-f) model the 28 February 1972 burst using L=0.9 AU and f_{pe}=60 KHz.

Figure 6. Results at 0.1 AU for two bursts. In panels (a-c) the 25 May 1972 burst is modeled using L=0.1 AU and f_{pe}=220 KHz. Panels (d-f) model the 28 February 1972 burst using L=0.2 AU and f_{pe}=300 KHz. Note that stabilization again proceeds via the OTSI and reabsorption is unimportant.

Figure 7. γ_{OTS} versus $W(k_o)$ from equation (III-3.28). Note the approximate scaling relations for $W_T<W(k_o)<m/M$ and $W(k_o)>m/M$.

Figure 8. After Fitzenreiter et al. (1976). The electron flux and power exponent, α from the relationship $I \propto J_E^{\alpha}$ are shown for the three events for which numerical calculations could be performed. Observed and computed values of α are plotted.

REFERENCES

Achong, A. A. and Barrow, C. H. 1975, Solar Phys., 45, 467.

Aubier, M. G. 1974, Astron. Astrophys., 32, 141.

Degtyarov, L. M. Zakharov, V. E., and Rudakov, L. I. 1976, Sov. J. of Plasma Phys., 2, 240.

Eiserike, H. M. and Silver, A. D. 1971, NASA Preprint X-641-70-199, NASA/Goddard Space Flight Center, Greenbelt, MD.

Fitzenreiter, R. J., Evans, L. G., and Lin, R. P. 1976 Solar Phys., 46, 437.

Gurnett, D. A. and Anderson, R. 1976, Science, 194, 1159.

Gurnett, D. A. and Anderson, R. 1977, J. Geophys. Res., 82, 632.

Gurnett, D. A. and Frank, L. A. 1975, Solar Phys., 45, 477.

Harvey, C. C., and Aubier, M. G. 1973, Astron. Astrophys., 22, 1.

Jaeger, J. C. and Westfold, K. C. 1949, Austral. J. Sci. Res., A2, 322.

Kingsep, A. S., Rudakov, L. I., and Sudan, R. N. 1973, Phys. Rev. Lett., 31, 1482.

Lin, R. P. 1974, Sp. Sci. Rev., 16, 189.

Lin, R. P., Evans, L. G., and Fainberg, J. 1973, Ap. Letters, 14, 191.

Magelseen, G. R. and Smith, D. F. 1977, Solar Phys., 55, 211.

Malville, J. M. 1962, Ap. J., 136, 266.

Manheimer, W. M., and Papadopoulos, K. 1975, Phys. Fluids, 18, 1397.

Papadopoulos, K. 1975, Phys. Fluids, 18, 1769.

Papadopoulos, K. and Freund, H. 1978, Geophys. Res. Lett., 5, 881.

Papadopoulos, K., Goldstein, M. L., and Smith, R. A. 1974, Ap. J., 190, 175.

Rowland, H. L. 1977, Ph. D. Thesis, Univ. of Maryland, College Park, MD.

Rudakov, L. I. 1973, Sov. Phys. Doklady, 17, 1166.

Smith, R. A., Goldstein, M. L., and Papadopoulos, K. 1976, Solar Phys., 46, 515.

Smith, R. A., Goldstein, M. L., and Papadopoulos, K. 1979, Ap. J., submitted.

Takakura, T. 1977, Solar Phys., 56, 429.

Takakura, T. and Shibahashi, H. 1976, Solar Phys., 46, 323.

Zaitsev, V. V., Mityakov, N. A., and Rappoport, V. O. 1972, Solar Phys., 24, 444.

Zakharov, V. E. 1972, Sov. Phys.--JETP, 35, 908.

TABLE CAPTIONS

TABLE I. Tabulation of the parameters used in the numerical integration of the rate equations (III-3.44) - (III-3.47).

TABLE I

Date of Burst	Heliocentric Radius of Calculation (AU)	Path Length L (AU)	Plasma Frequency f_{pe} (KHz)	$\eta_i = n_b/n$	Electron Spectral Index ζ	Solar Wind Electron Temperature (10^{5o}K)	Figure Showing Results
May 16, 1971	1	1.5	30	5×10^{-6}	4.6	1.2	2 (a-f)
	0.5	0.7	60				4 (a-c)
	0.1	0.1	300				4 (d-e)
February 28, 1972	1	1.9	30	1.4×10^{-4}	10.4	1.2	3 (a-c)
	0.5	0.9	60				5 (d-f)
	0.1	0.2	300				6 (a-c)
May 25, 1972	1	1.5	22	5.6×10^{-5}	6.4	1.2	3 (d-f)
	0.5	0.7	44				5 (a-c)
	0.1	0.1	220				6 (d-f)

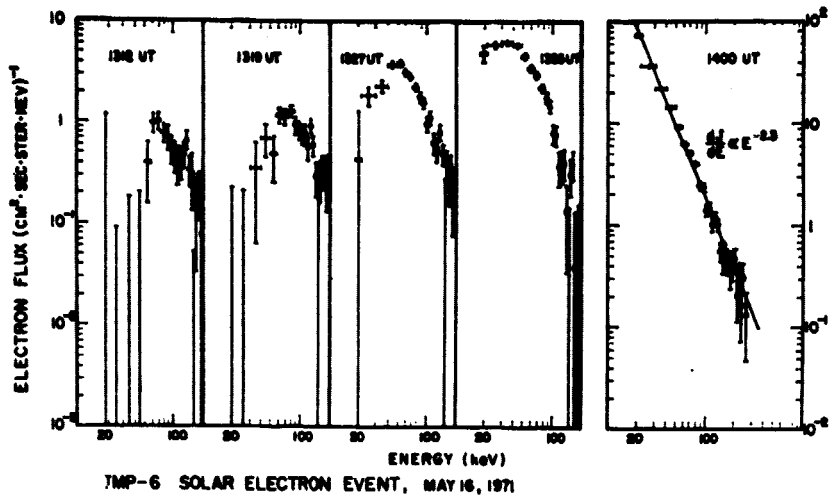
ELECTRON FLUX (cm²·sec·ster·kev)⁻¹
1340 UT
1349 UT
1400 UT
ENERGY (keV)
IMP-6 SOLAR ELECTRON EVENT, MAY 16, 1971

Figure 1

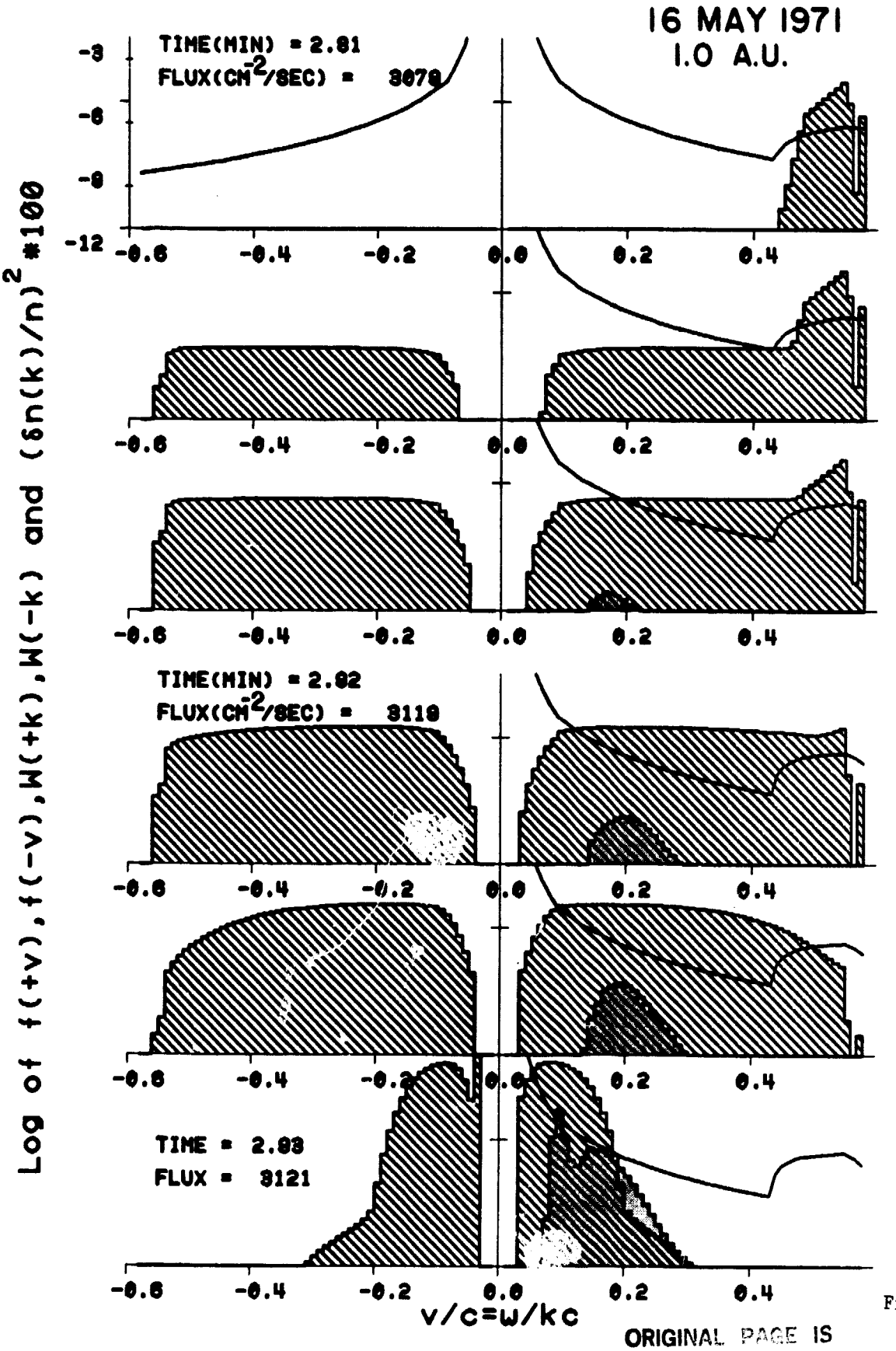

Figure 2

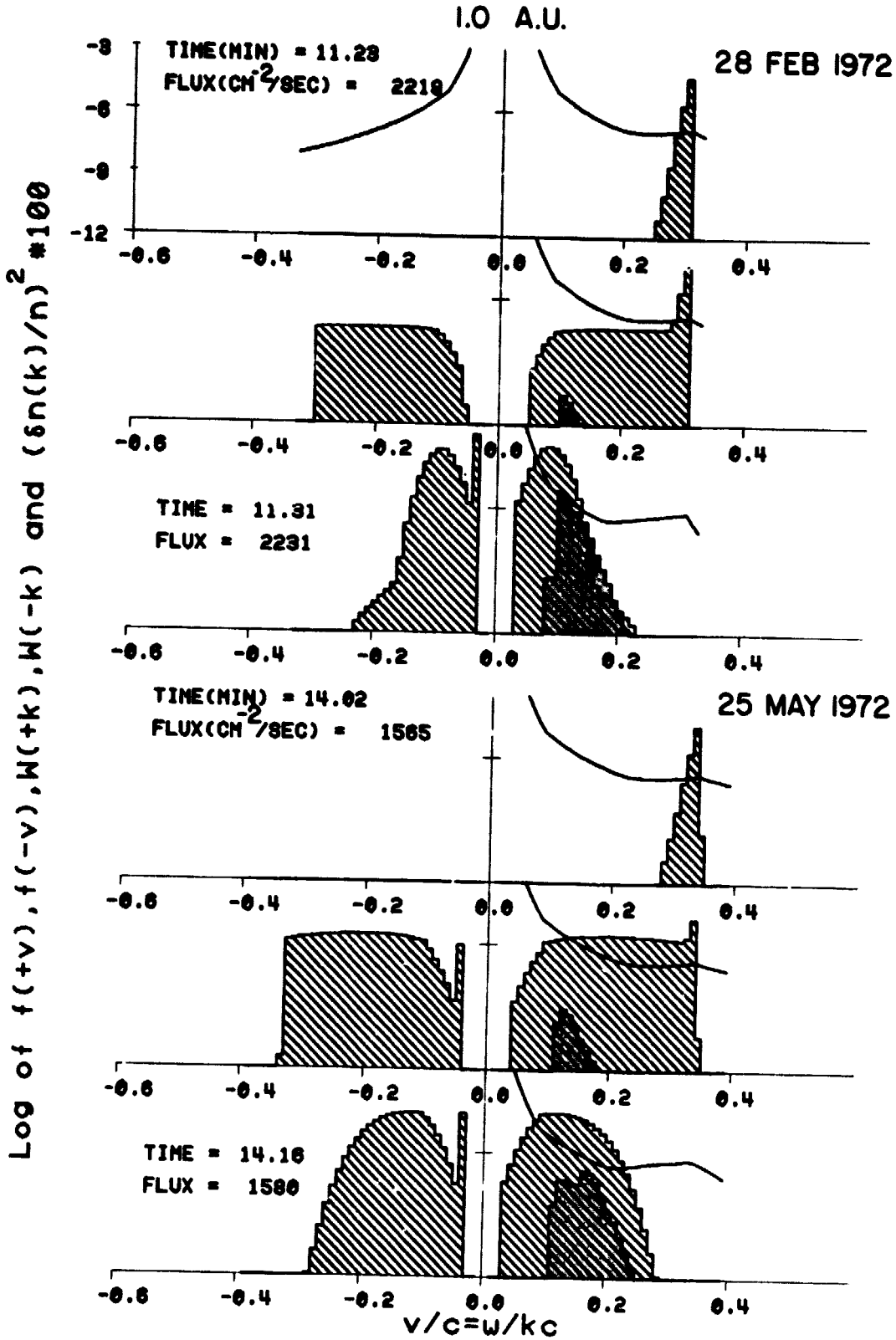

Figure 3

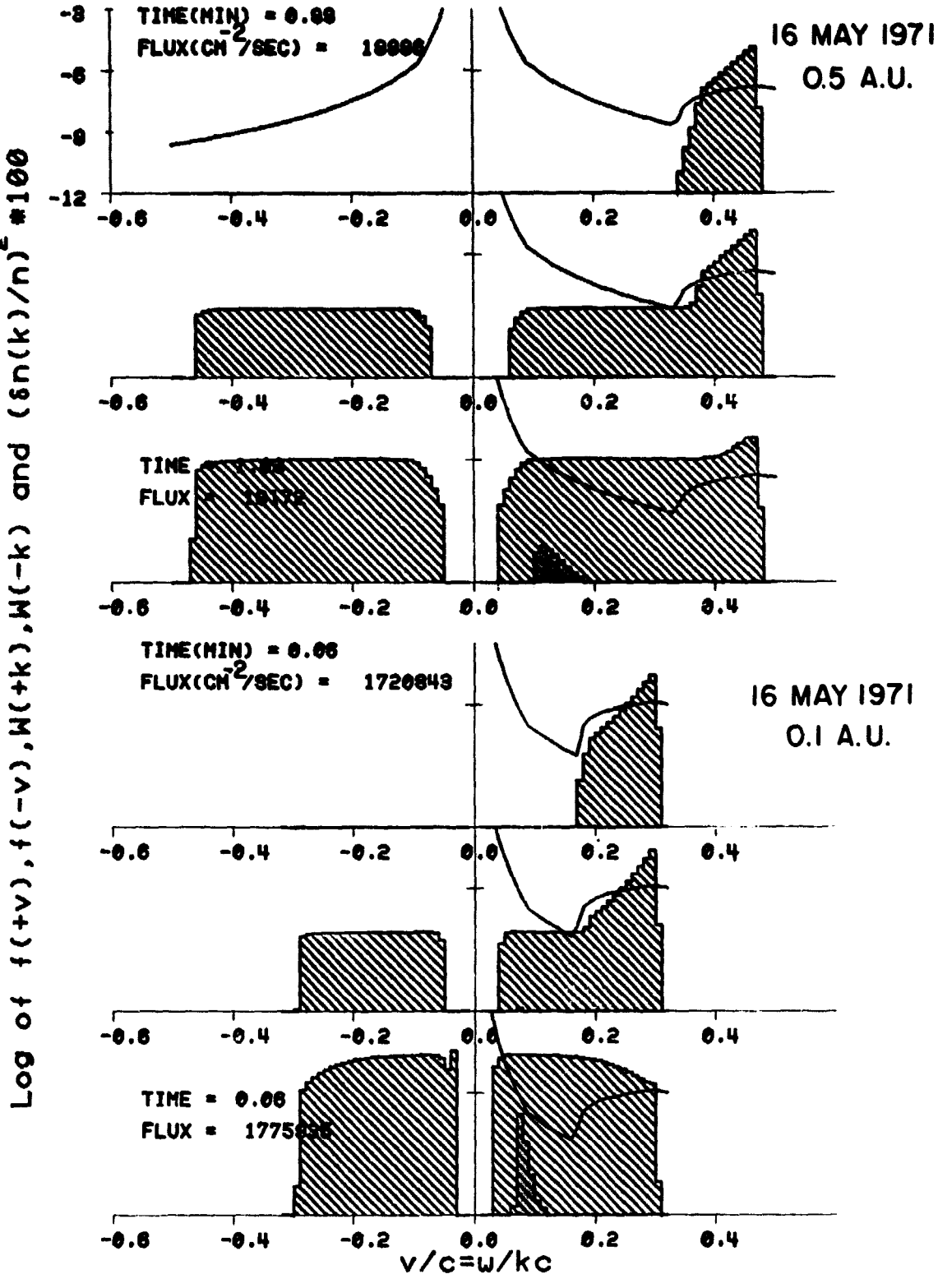
16 MAY 1971
0.5 A.U.
16 MAY 1971
0.1 A.U.
v/c=w/kc
Log of f(+v), f(-v), W(+k), W(-k) and (δn(k)/n)² *100

Figure 4

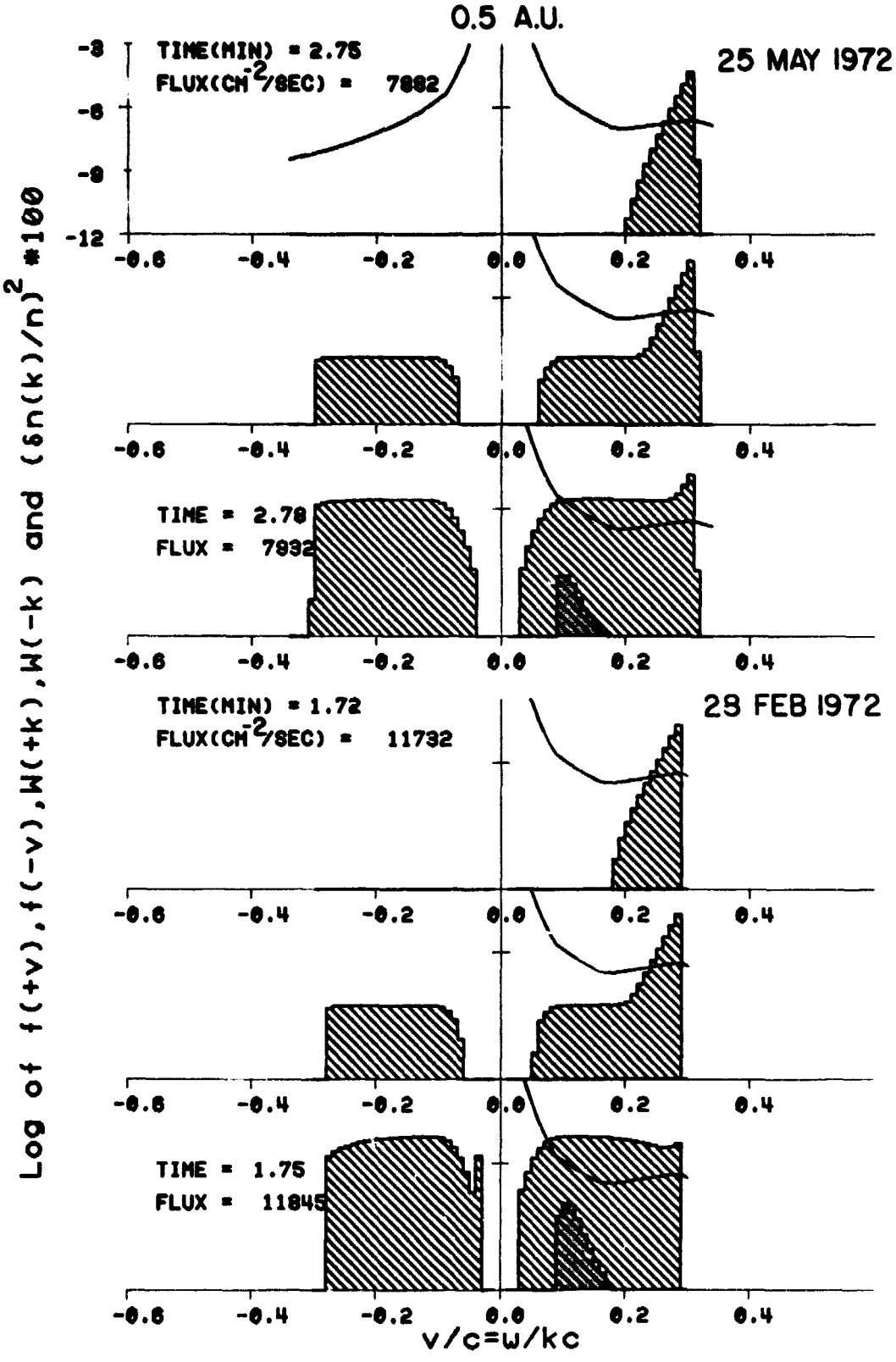

Figure 5

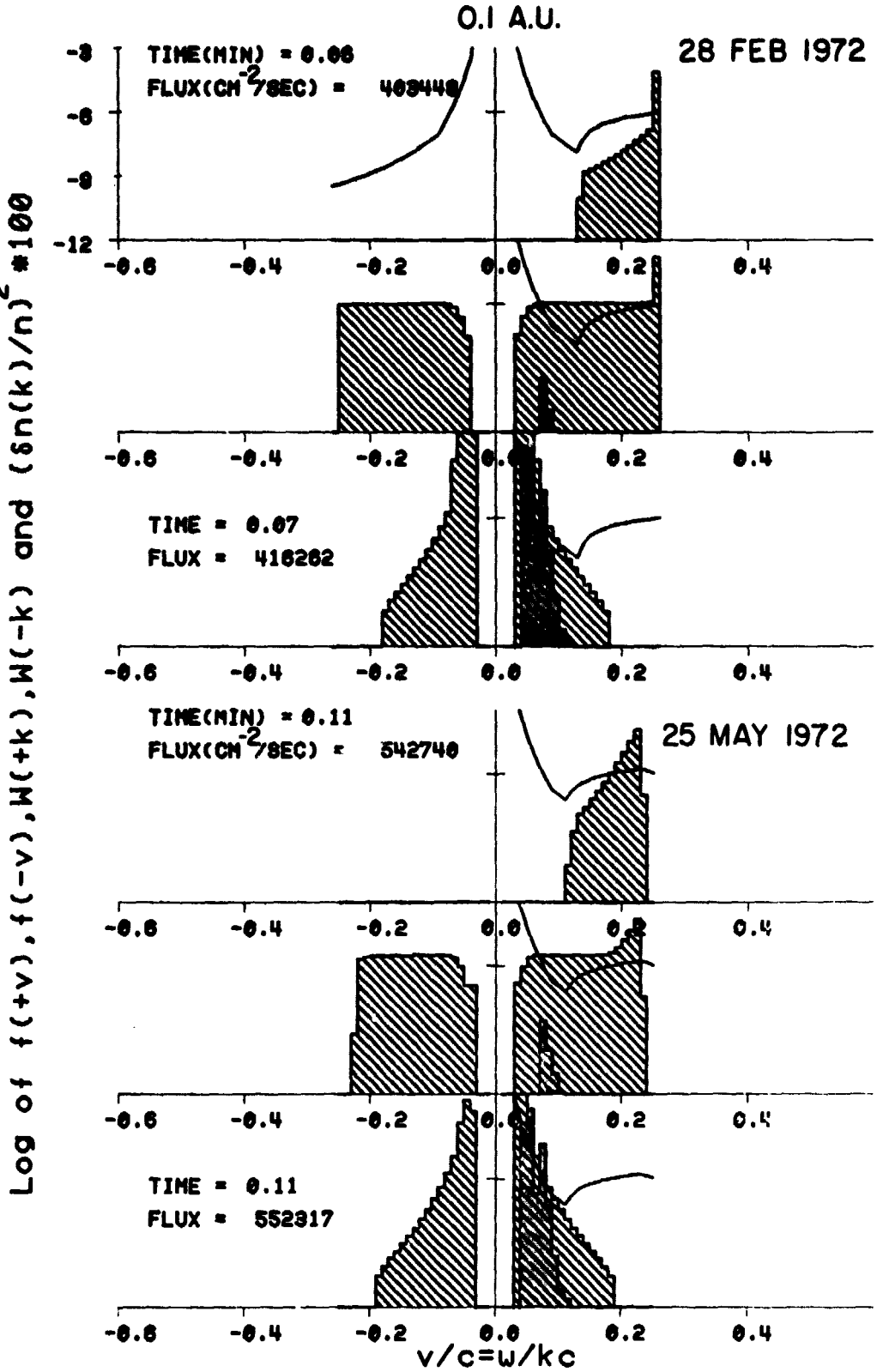
0.1 A.U.
28 FEB 1972
TIME(MIN) = 0.06
FLUX(CM-2 SEC) = 403448
TIME = 0.07
FLUX = 416262
25 MAY 1972
TIME(MIN) = 0.11
FLUX(CM-2 SEC) = 542740
TIME = 0.11
FLUX = 552317
-8
-6
-8
-12
-0.6
-0.4
-0.2
0.0
0.2
0.4
Log of f(+v),f(-v),W(+k),W(-k) and (δn(k)/n)2 *100
v/c=w/kc

Figure 6

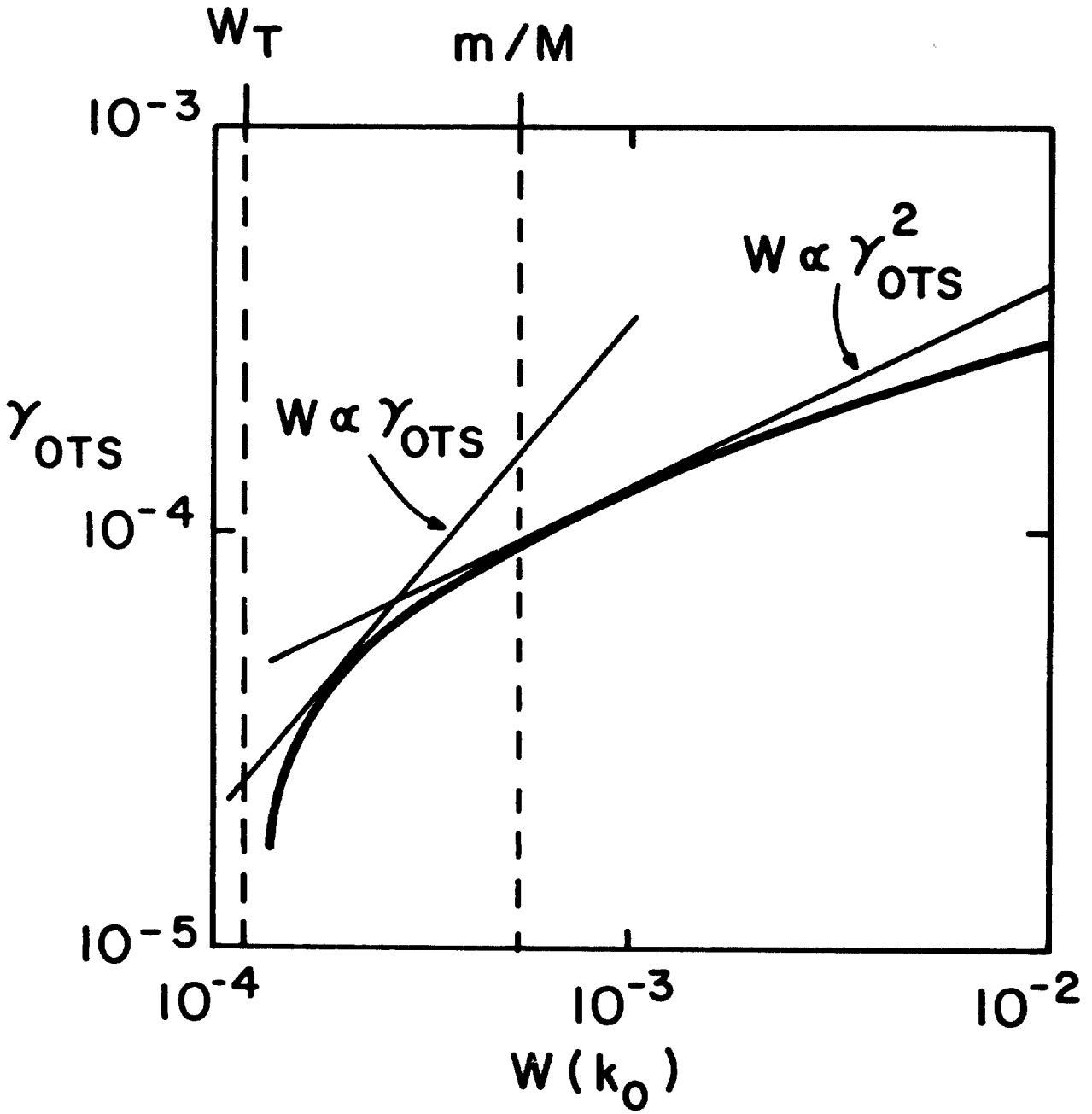
W_T
m/M
10^{-3}
10^{-4}
10^{-5}
γ_{OTS}
$W \propto \gamma_{OTS}$
$W \propto \gamma_{OTS}^2$
10^{-4}
10^{-3}
10^{-2}
$W(k_0)$

Figure 7

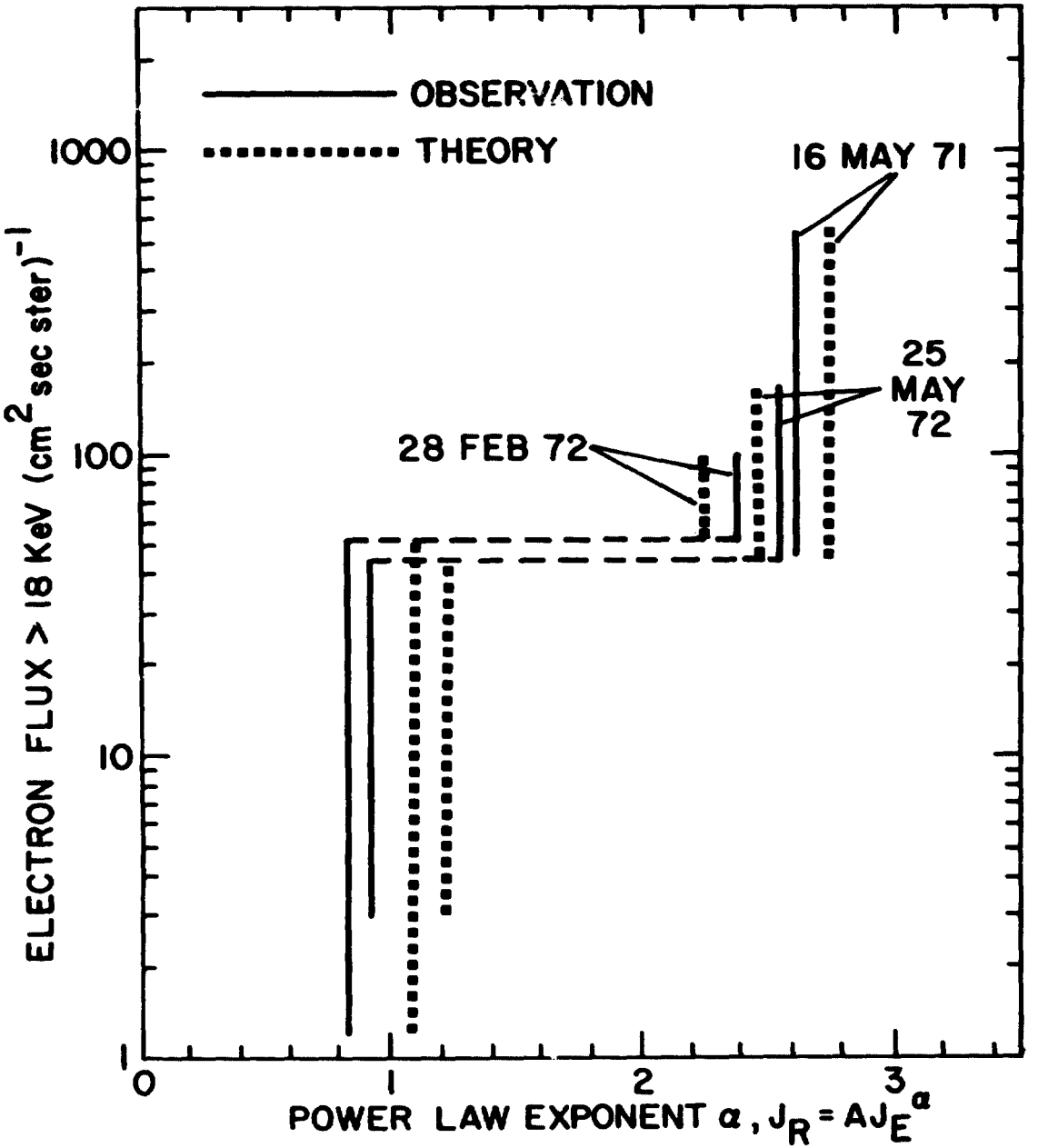
OBSERVATION
THEORY
16 MAY 71
25
MAY
72
28 FEB 72
1000
100
10
1
0
1
2
3
ELECTRON FLUX > 18 KeV (cm^2 sec ster)$^{-1}$
POWER LAW EXPONENT α, $J_R = AJ_E^{\alpha}$

Figure 8